Defect-controlled halogenating properties of lanthanide-doped ceria nanozymes

Phil Opitz,[1‡] Olga Jegel,[1‡] Jamal Nasir,[2] Tobias Rios-Studer,[1] Athanasios Gazanis,[3] Dang-Hieu Pham,[1] Katrin Domke,[4] Ralf Heermann,[3] Jörn Schmedt auf der Günne,[2*] Wolfgang Tremel[1*]

[1] Johannes Gutenberg-Universität Mainz, Department Chemie, Duesbergweg 10-14, D-55128 Mainz, Germany, tremel@uni-mainz.de

[2] University of Siegen, Faculty IV: School of Science and Technology, Department of Chemistry and Biology, Adolf-Reichwein-Straße 2, D-57076 Siegen, Germany, gunnej@chemie.uni-siegen.de

[3] Johannes-Gutenberg-Universität Mainz, Institut für Molekulare Physiologie, Biozentrum II, Mikrobiologie und Biotechnologie, Hanns-Dieter-Hüsch-Weg 17, 55128 Mainz, Germany, heermann@uni-mainz.de

[4] Max-Planck-Institut für Polymerforschung, Ackermannweg 10, D-55128 Mainz, Germany

Table of Contents

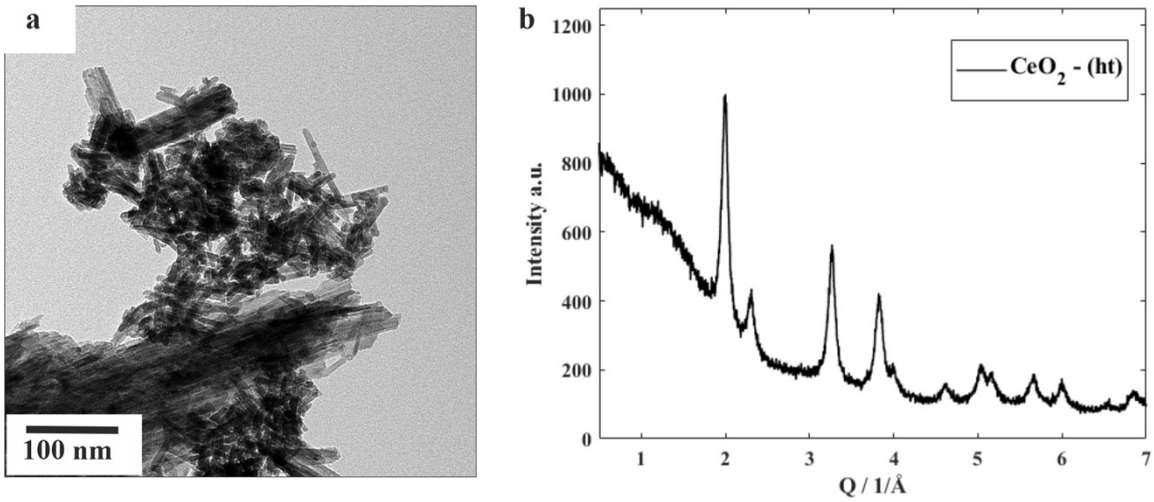

Fig. S1. a) TEM image and b) X-ray diffractogram of hydrothermally prepared CeO_2 nanocrystals.

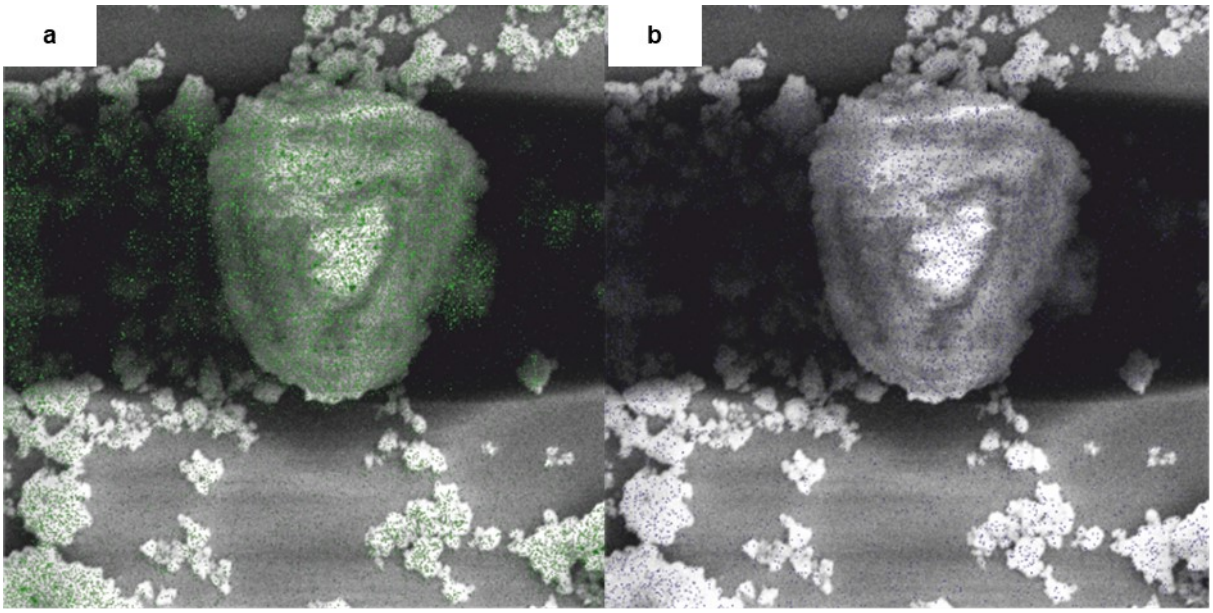

Fig. S2. SEM EDX mapping of Tb-doped CeO_2 nanocrystals. a) X-rays for the Ce L line b) X-rays for the Tb L line.

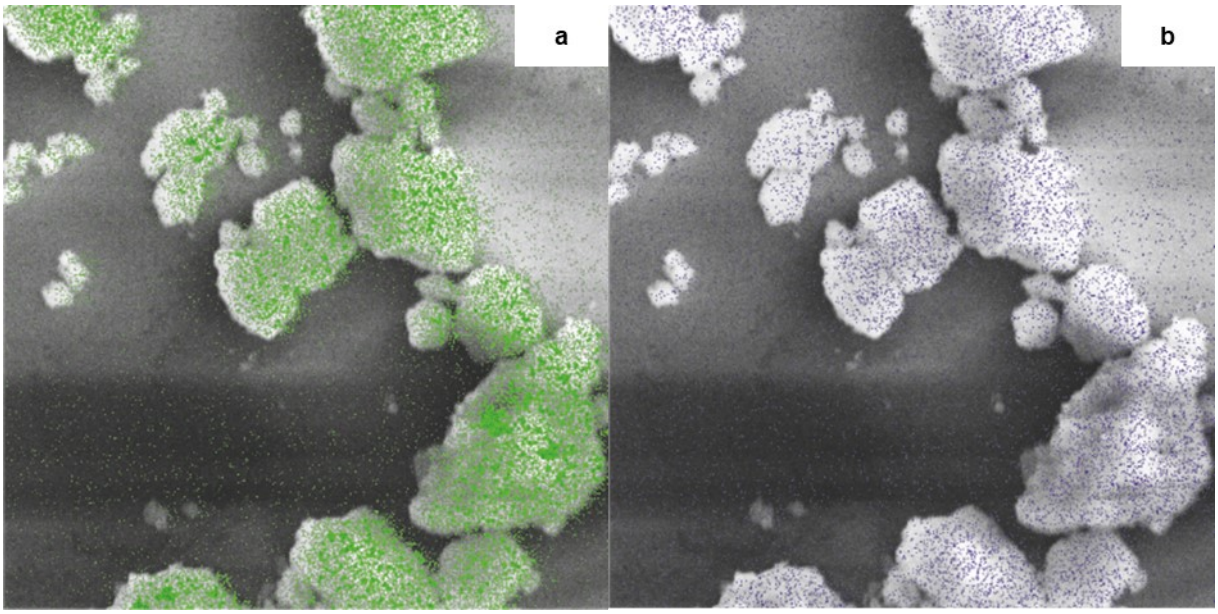

Fig. S3. SEM EDX mapping of the Pr-doped nanocrystals. a) X-rays for the Ce L line b) X-rays for the Pr L line.

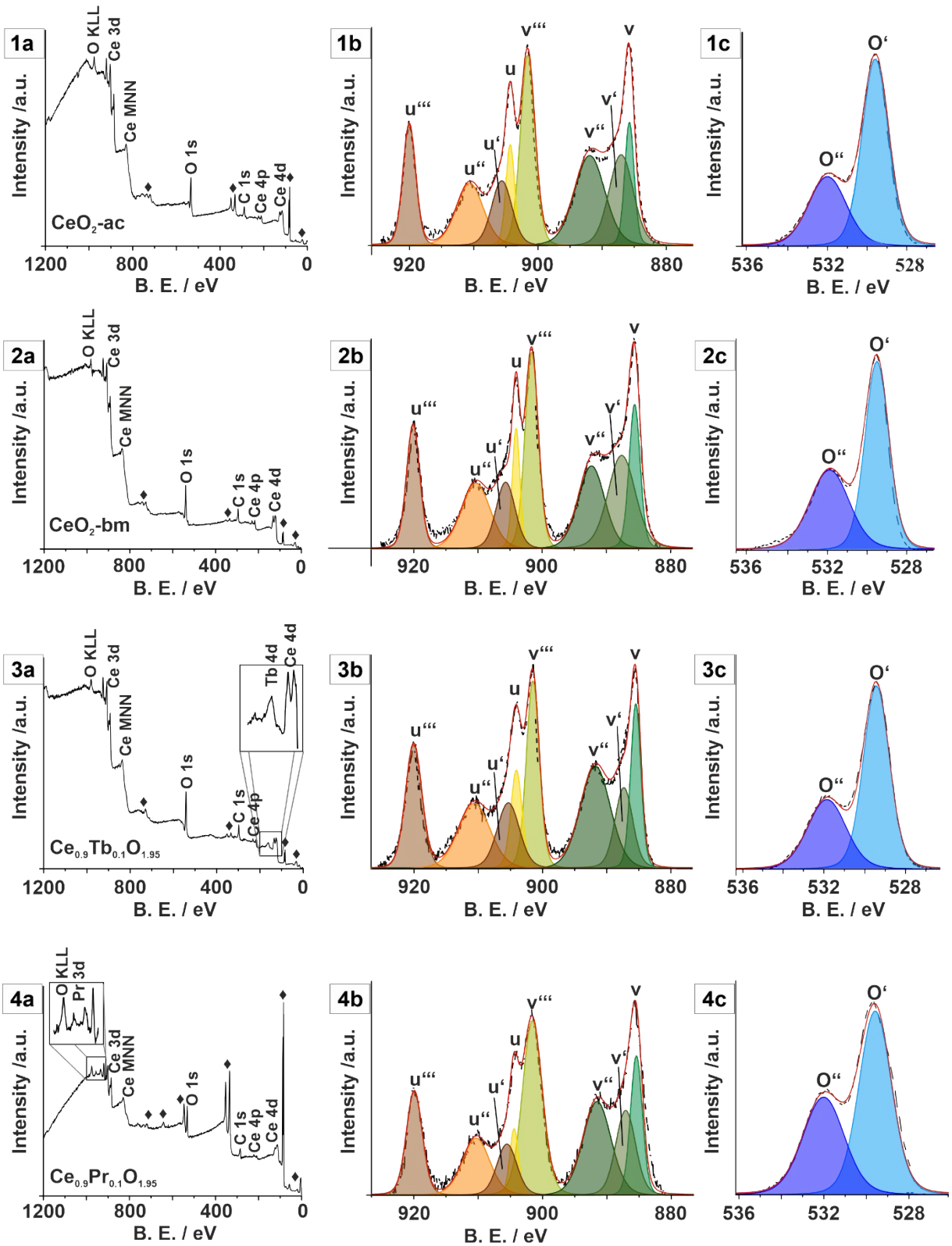

Fig. S4. X-ray photoelectron spectroscopy spectra of CeO_2-ht (1), CeO_2-bm (2), $Ce_{0.9}Tb_{0.1}O_{1.95}$ (3) and $Ce_{0.9}Pr_{0.1}O_{1.95}$ (4). a) Survey spectra. b) Ce 3d and c) the O 1s regions.[1-3]

Table S1. Table of the signal positions in XPS survey spectra in Fig. S4.

Peak Energy / eV	Element	Peak Assignment	Shortcut
40	Au 5p	-	♦
85	Au 4f		♦
88	Au 4f	-	♦
122	Ce 4d	Ce(IV) in CeO_2	-
125	Ce 4d	Ce(IV) in CeO_2	-
155	Tb 4d	-	-
285	C 1s	-	-
~340	Au 4d	-	♦
~355	Au 4d	-	♦
530	O 1s	Ce(IV)-O	O’
532	O 1s	Ce(III)-O and adsorbed – CO_3^{2-} species	O’’
~560	Au 4p	-	♦
~650	Au 4p	-	♦
~770	Au 4s	-	♦
883	Ce $3d_{5/2}$	Ce(IV) in CeO_2	v
885	Ce $3d_{5/2}$	Ce(III) in CeO_{2-x}	v’
889	Ce $3d_{5/2}$	Ce(IV) in CeO_2	v’’
899	Ce $3d_{5/2}$	Ce(IV) in CeO_2	v’’’
901	Ce $3d_{3/2}$	Ce(IV) in CeO_2	u
904	Ce $3d_{3/2}$	Ce(III) in CeO_{2-x}	u’
908	Ce $3d_{3/2}$	Ce(IV) in CeO_2	u’’
917	Ce $3d_{3/2}$	Ce(IV) in CeO_2	u’’’
933	Pr $3d_{5/2}$	-	-
954	Pr $3d_{3/2}$	-	-

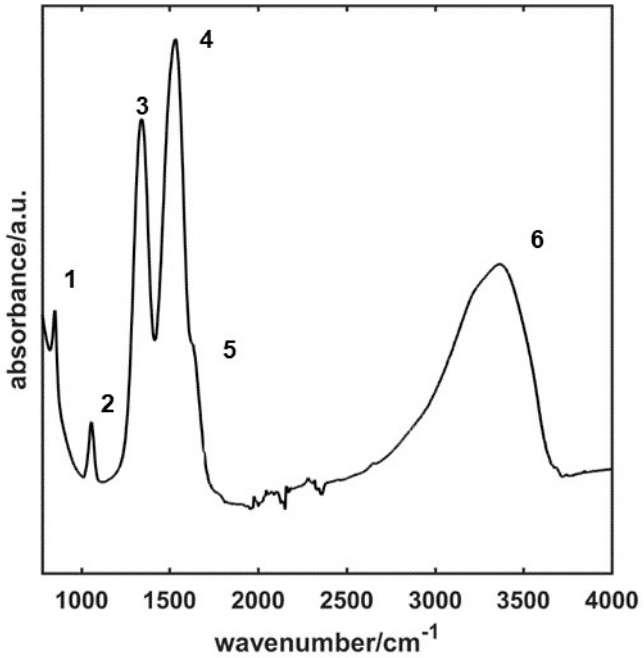

Fig. S5. FTIR spectrum of ball milled CeO_2. The bands marked with numbers are shown in Table S1.

Table S2. Assignment of the FTIR vibrational bands. The first five bands are assigned to chemisorbed CO_2. The sixth broad band is assigned to OH groups of free and adsorbed water.

No. of FTIR band	Position(cm^{-1})	Assignments[4-6]
1	851	Out of-plane vibration of the surface carbonate CO_3^{2-} group,
2	1058	unidentate CO_3^{2-}
3	1341	unidentate CO_3^{2-}
4	1534	bidentate CO_3^{2-}
5	1633	bending vibration of water
6	2800-3650	υ_{-OH} of free, adsorbed and chemisorbed water

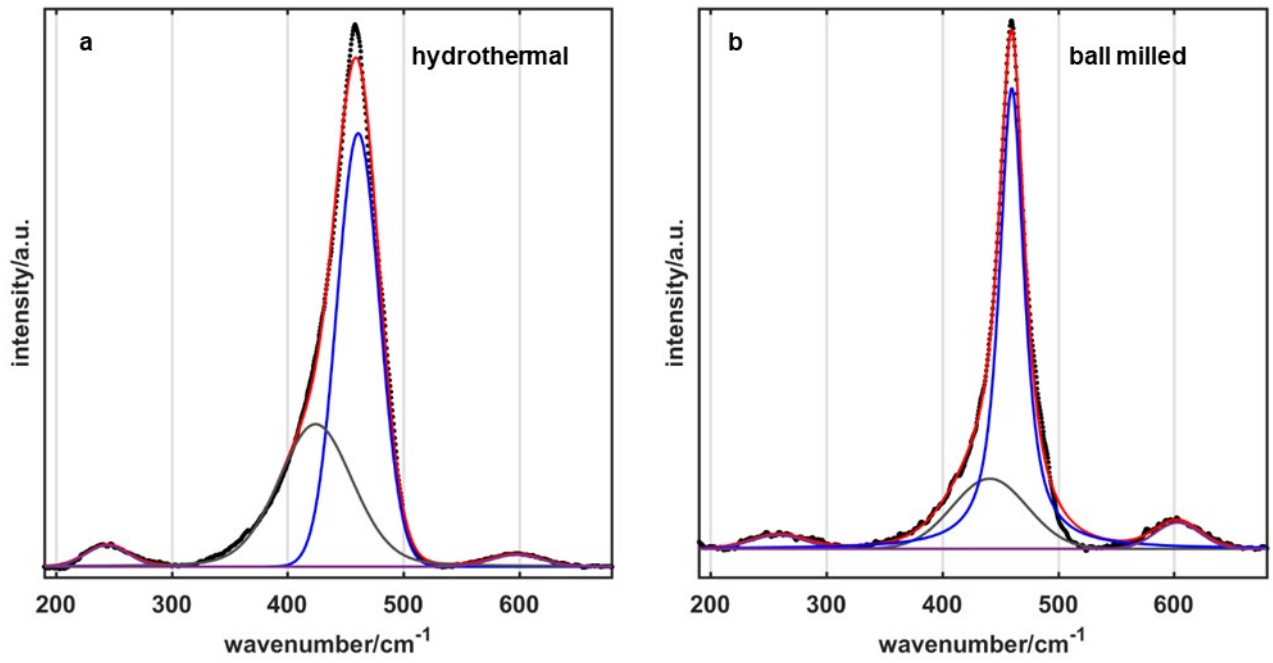

Fig. S6. Best Lorentz fit (red line) of the Raman spectra of CeO_2 nanocrystals synthesized (a) hydrothermally and (b) by ball milling. The full width at half maximum (fwhm) of the main band (43.3 cm^{-1}) of the hydrothermally prepared CeO_2 nanocrystals is significantly larger than the band (25.7 cm^{-1}) of the ball-milled nanocrystals. This indicates a higher disorder of hydrothermally prepared nanocrystals and is most probably explained by the anisotropic crystal morphology.

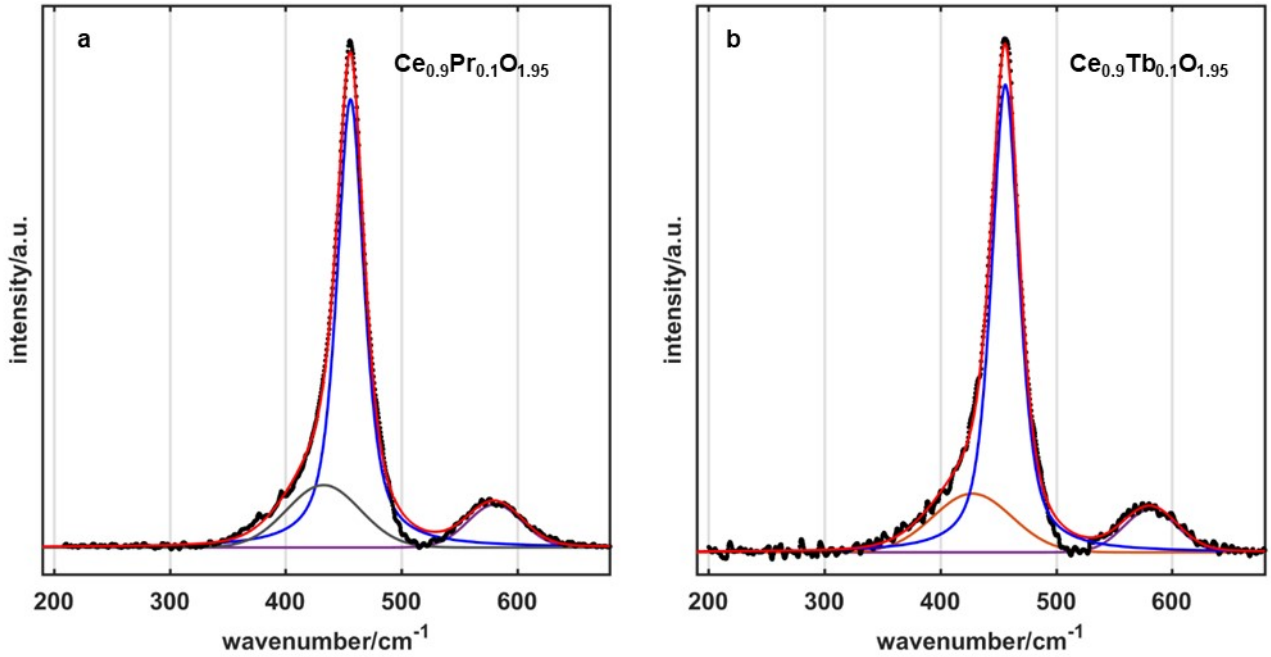

Fig. S7. Best Lorentz fit (red line) of the Raman spectra of the (a) Pr- and (b) Tb-doped CeO_2 nanocrystals.

Table S3. Assignment of Raman spectra.

	Band 1(cm^{-1})	Band 2 (cm^{-1})	Band 3(cm^{-1})	Band 4(cm^{-1})
CeO_2 hydrothermally prepared	244.2	424.2	461.0	598.0
CeO_2 ball milled	258.3	440.9	460.0	603.0
$Ce_{0.9}Pr_{0.1}O_{1.95}$	-	432.8	456.1	580.9
$Ce_{0.9}Tb_{0.1}O_{1.95}$	-	427.7	456.1	581.4
Assignments[7-10]	TA/TO	F_{2g}	F_{2g}	D_1

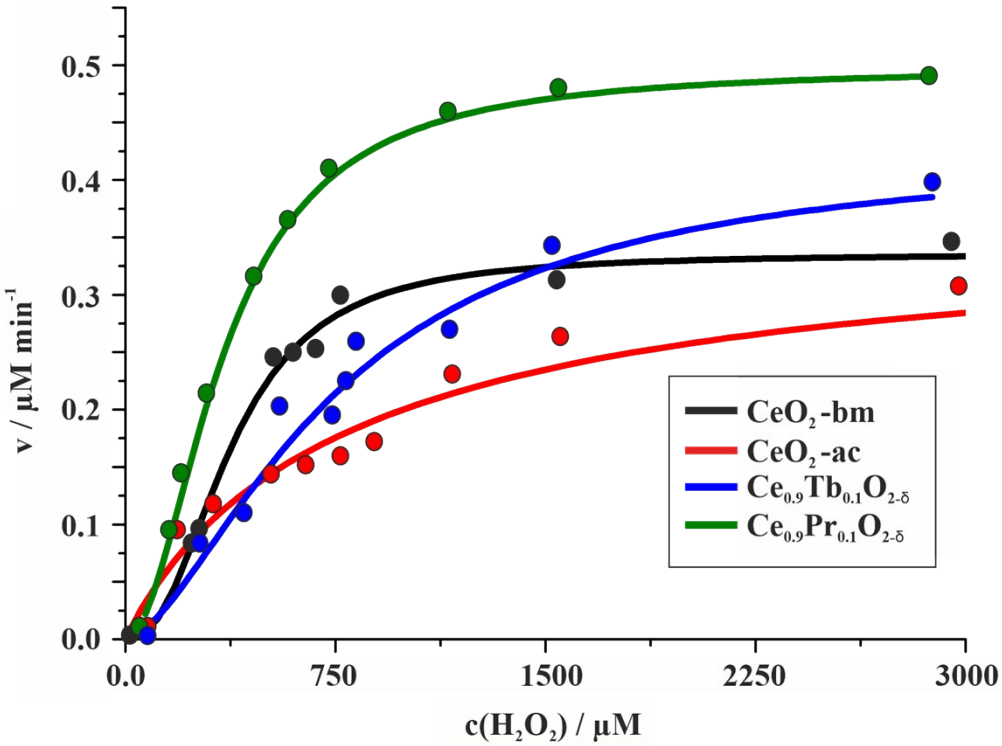

Fig. S8. Hill-Fit of undoped and Pr- and Tb-doped CeO_2 nanocrystals.

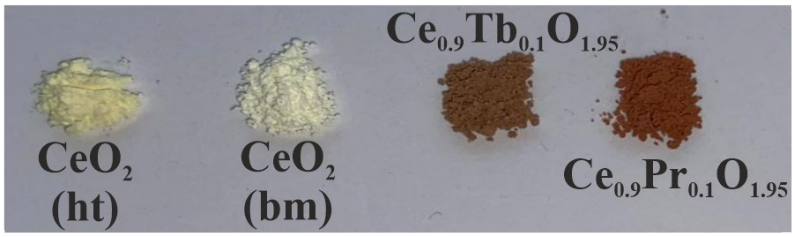

Fig. S9. Digital photographs of CeO_2 (bm and ht), $Ce_{0.9}Tb_{0.1}O_{1.95}$ and $Ce_{0.9}Pr_{0.1}O_{1.95}$ powders.

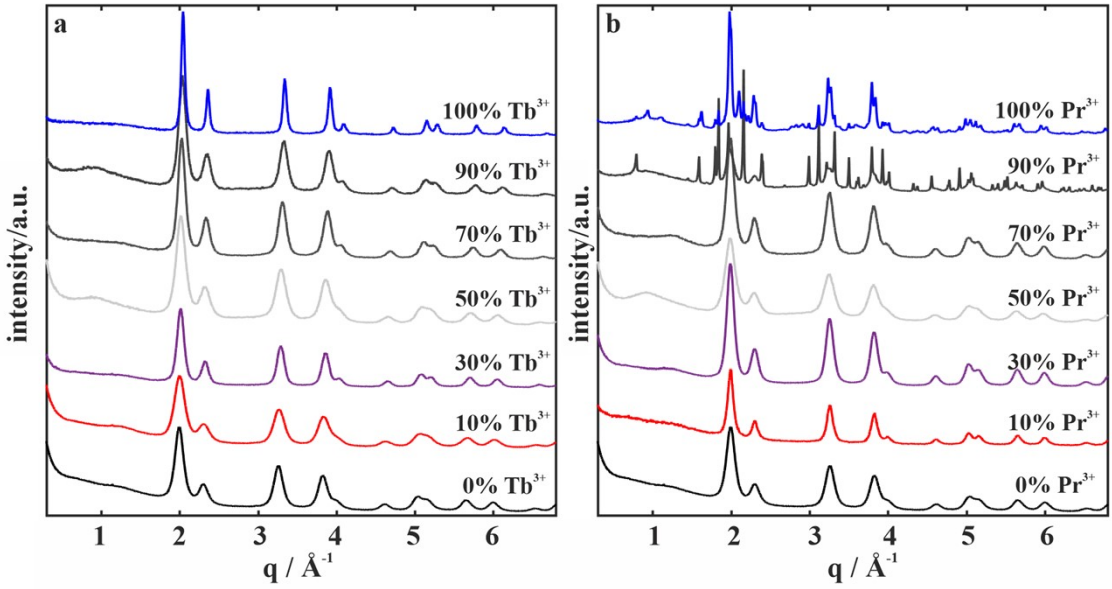

Fig. S10. X-ray powder diffractograms showing the miscibility of CeO_2 with a) (Tb^{3+}) and b) (Pr^{3+}).

References

(1) R. Valiokas, L. Malysheva, A. Onipko, H.-H. Lee, Z. Ruzele, S. Svedhem, S. C.T. Svensson, U. Gelius, B. Liedberg, *J. Electr. Spectr. Rel. Phenom*. 2009, **172**, 9–20

(2) M. M. Natile and A. Glisenti, *Surf. Sci. Spectra* 2006 **13**, 17.

(3) Y. Sohn, *Ceram. Int.* 2014, **40**, 13803-13811.

(4) C. Li, Y. Sakata, T. Arai, K. Domen, K. Maruya, T. Onishi, *J. Chem. Soc., Faraday Trans.* 1989, **85**, 929.

(5) S. Chen, T. Cao, Y. Gao, D. Li, F. Xiong, W. Huang, *J. Phys. Chem. C* 2016, **120**, 21472–21485.

(6) G. N. Vayssilov, M. Mihaylov, P. S. Petkov, K. I. Hadjiivanov, K. M. Neyman, *J. Phys. Chem. C* 2011, **115**, 23435–23454.

(7) W. H. Weber, K. C. Hass, J. R. McBride, *Phys. Rev. B* 1993, **48**, 178–185.

(8) C. Schilling, A. Hofmann, C. Hess, M. Veron, *J. Phys. Chem. C* 2017, **16**, 20834–20849.

(9) O. Kraynis, I. Lubomirsky, T. Livneh, *J. Phys. Chem. C* 2019, **123**, 24111–24117.

(10) M. Gupta, A. Kumar, A. Sagdeo, P. R. Sagdeo, *J. Phys. Chem. C* 2021, **125**, 2648–2658.